

## Alternative transfer-matrix approach to two-dimensional systems with competing interactions in one direction

Marcelo D. Grynberg and Horacio Ceva

*División Física del Sólido, Comisión Nacional de Energía Atómica, Avenida del Libertador 8250, 1429 Buenos Aires, Argentina*

(Received 9 February 1987)

A transfer-matrix representation in terms of Pauli spin matrices is used to perform a phenomenological renormalization and finite-size scaling analysis of two-dimensional spin models with competing interactions in one direction. This enables us to obtain the leading eigenvalues of the transfer matrix with a significative saving of computer time using the Lanczos scheme. The phase diagrams of the axial next-nearest-neighbor Ising model and a model with competing two- and four-spin couplings in one direction are studied. The order of the phase transitions was determined by examining the finite-size scaling behavior of the persistence length. Data for the normalized scaled persistence length display scaling on the ferromagnetic-paramagnetic transition line for both models.

### I. INTRODUCTION

Two-dimensional spin systems with competing interactions along one direction have been extensively studied in recent years.

These models exhibit a variety of characteristic effects which are reflected in the complexity of their phase diagrams.

The axial next-nearest-neighbor Ising (ANNNI) model<sup>1</sup> and a multispin model with competing two- and four-spin couplings in one direction (2+4 model), introduced recently by Penson,<sup>2</sup> are two examples of such models.

Many calculations have already been performed on these models; examples of these are one-dimensional quantum Hamiltonian versions<sup>3</sup> using finite-size scaling (FSS) methods, Monte Carlo simulations,<sup>4</sup> interface free-energy calculations,<sup>5</sup> and a free-fermion approximation.<sup>6</sup>

All of them display the same type of phases, although the phase boundaries are conspicuously different, mainly in the neighborhood of the point where the ground state of these models is infinitely degenerate.

In this article we exploit an alternative derivation of the transfer matrix, which was originally applied by Schultz *et al.*<sup>7</sup> to the two-dimensional Ising model. This technique is easily generalized to two-dimensional models with complex interactions in one direction.

Using this methodology we present a phenomenological renormalization (PR) and FSS analysis<sup>8</sup> of the ANNNI and the 2+4 models.

The third eigenvalue of the transfer matrix gives a measure of the interface free energy between the different phases which coexist at a transition line<sup>9</sup> and then provides information as to whether the transition is continuous or first order.

### II. THE TRANSFER MATRIX

In a classical paper, Schultz *et al.*<sup>7</sup> solved the two-dimensional Ising model by means of a free-fermion for-

mulation of the model. The heart of their method is an alternative derivation of the transfer matrix.

We use this approach to write the partition function of a general two-dimensional model system consisting of  $M$  rows and  $N$  columns of spins  $s = \pm 1$  and interactions  $J_i$ , with Hamiltonian

$$\beta\mathcal{H} = -K_0 \sum_{m,n} \sigma_{mn}^x \sigma_{m+1,n}^x - K_1 \sum_{m,n} \sigma_{mn}^x \sigma_{m,n+1}^x - H \sum_{m,n} \sigma_{mn}^x - \sum_m \hat{\mathcal{O}}_m \{ \sigma_n^x, h_n \}, \quad K_1 > 0 \quad (1)$$

where  $\beta = 1/k_B T$ ,  $K_i = \beta J_i$ , and  $\sigma_{mn}^x$  is the usual Pauli spin matrix for the  $(m,n)$  site of the lattice,  $H$  is the reduced magnetic field, and  $\hat{\mathcal{O}}_m$  is a very general type of row interaction which can include any combination of spins  $s$  and fields  $h$  on the same row and  $\sigma_n^x$  the Pauli spin matrix for the  $n$  site of an arbitrary row.

In the ANNNI model we have

$$\hat{\mathcal{O}}_{\text{ANNNI}} \{ \sigma_n^x; h_n = 0 \} = -K_2 \sum_n \sigma_n^x \sigma_{n+2}^x, \quad K_2 > 0. \quad (2)$$

In the 2+4 or multispin model,  $\hat{\mathcal{O}}_{2+4}$  is written as

$$\hat{\mathcal{O}}_{2+4} \{ \sigma_n^x; h_n = 0 \} = -K_4 \sum_n \sigma_n^x \sigma_{n+1}^x \sigma_{n+2}^x \sigma_{n+3}^x, \quad K_4 > 0. \quad (3)$$

Following the method of Ref. 7, it is possible to write the partition function in terms of a single-row state,  $|0\rangle$ , which has all their spins  $s = -1$ , as

$$Z = \langle 0 | (V_H V_{\hat{\mathcal{O}}} V_1 V_0)^M | 0 \rangle. \quad (4)$$

The result of Schultz *et al.* for the Ising model corresponds to the case  $V_{\hat{\mathcal{O}}} = 1$ . The  $V$ 's are  $2^N \times 2^N$  matrices given by

$$\begin{aligned} V_H &= \exp \left[ H \sum_n \sigma_n^x \right], \\ V_{\hat{\mathcal{O}}} &= \exp \left[ \hat{\mathcal{O}} \right], \\ V_1 &= \exp \left[ K_1 \sum_n \sigma_n^x \sigma_{n+1}^x \right] \\ V_0 &= (2 \cosh K_0)^N (\tanh K_0)^{\hat{N}}, \end{aligned} \quad (5)$$

where  $\hat{N}$  is the row number operator written in terms of spin-raising and -lowering operators:

$$\hat{N} = \sum_n \sigma_n^+ \sigma_n^- . \quad (6)$$

For computational purposes it is convenient to rewrite  $Z$  as

$$Z = \langle 0 | V_0^{-1/2} (\hat{T})^M V_0^{1/2} | 0 \rangle , \quad (7)$$

where  $\hat{T}$  is the Hermitian transfer matrix:

$$\hat{T} = V_0^{1/2} V_H V_{\hat{O}} V_1 V_0^{1/2} . \quad (8)$$

If there were other interactions between rows besides the assumed nearest-neighbor constant coupling, the hermiticity of  $\hat{T}$  would be lost.

It is easy to show that in terms of the eigenfunctions  $|\varphi_j\rangle$  and eigenvalues  $\lambda_j$  ( $\lambda_1 > \lambda_2 > \dots$ ) of the transfer matrix  $Z$  can be written as

$$Z = \sum_j \lambda_j^M |\langle 0 | \varphi_j \rangle|^2 . \quad (9)$$

If  $M \rightarrow \infty$ , it is clear that the free energy per spin,  $f$ , is

$$f = -\frac{T \ln Z}{MN} \rightarrow -\frac{T \ln \lambda_1}{N} \quad \text{as } M \rightarrow \infty , \quad (10)$$

where  $\lambda_1$  is the maximum eigenvalue of  $\hat{T}$ .

With this notation, the correlation function between two spins in the same row is expressed as<sup>7</sup>

$$\begin{aligned} \langle \sigma_n^x \sigma_n^x \rangle &= \frac{\text{Tr}(V_0^{1/2} \sigma_n^x \sigma_n^x V_0^{-1/2} \hat{T}^M)}{\text{Tr} \hat{T}^M} \\ &\rightarrow \langle \varphi_{\max} | V_0^{1/2} \sigma_n^x \sigma_n^x V_0^{-1/2} | \varphi_{\max} \rangle \quad \text{as } M \rightarrow \infty , \end{aligned} \quad (11)$$

where  $|\varphi\rangle_{\max}$  denotes the eigenvector corresponding to the maximum eigenvalue.

In our case  $\hat{O}_{\text{ANNNI}}$  and  $\hat{O}_{2+4}$ , acting on any row state  $|s_1^z, s_2^z, \dots, s_N^z\rangle$ , characterized by the  $z$  component of the spins  $s$  (and  $H=0$ ), flip an even number of them. Hence, there are two invariant subspaces of dimension  $2^{N-1}$  containing, respectively, the eigenvalues  $\lambda_1, \lambda_3, \dots$  and  $\lambda_2, \lambda_4, \dots$ . This represents an important saving of computer time.

The main advantage of our approach with respect to other implementations of the transfer-matrix method is that we never need to actually construct the  $\hat{T}$  matrix. Instead, we have an operational representation of  $\hat{T}$  in terms of spin-raising and -lowering operators.

The Lanczös<sup>10</sup> scheme for searching the leading eigenvalues of  $\hat{T}$  is highly efficient when it is used with this approach.

Hence we only need to keep proper track of all spin flips produced by applications of  $\hat{T}$  to any row state (see the Appendix).

It is remarkable that, for  $N=12$ , few iterations (5–15) of the Lanczös process are sufficient to obtain the first three eigenvalues of  $\hat{T}$  with acceptable accuracy ( $10^{-5}$ – $10^{-6}$ ).

We used this technique to implement the phenomenological renormalization and FSS analysis in the standard form, for lattices up to  $N=12$  with periodic boundary conditions.

We were able to solve these models for  $N=12$  with a detailed study of their behavior as a function of temperature, using a few CPU hours on a VAX 11/780 computer.

The transfer-matrix formulation is intrinsically richer than the Hamiltonian formulation, because in the later case, it is only possible to study a highly anisotropic limit case.

Our phase diagrams have been studied mainly for  $K_0/K_1=1$ , but we also considered the behavior of these models for  $K_0/K_1=10, 50$ , and  $100$  for  $X < 0.5$ , where  $X$  measures the degree of competition:  $X=K_2/K_1$  ( $X=K_4/K_1$ ) for the ANNNI (2+4) model.

For the models we studied, there is a modulation along the direction of competitive interactions. The main drawback of our approach is due to the fact that this direction is, unfortunately, the finite one. This limits mainly our ability to study the wave vector of the modulation. It should be noticed that we always deal with  $2^N \times 2^N$  matrices, while an implementation with the modulation along the infinite direction has to deal with  $4^N \times 4^N$  and  $8^N \times 8^N$  matrices in the ANNNI and 2+4 models, respectively.

### III. RESULTS

#### A. Calculated magnitudes

In this work we calculated the following five magnitudes.

(i) Correlation length,<sup>9</sup>

$$\xi = 1 / \ln(\lambda_1 / \lambda_2) . \quad (12)$$

(ii) Scaling function,<sup>11</sup>  $Y(N, N')$ ,

$$Y(N, N') = \ln(\xi_N / \xi_{N'}) / \ln(N / N') , \quad (13)$$

where  $\xi_N$  ( $\xi_{N'}$ ) is the correlation length for a  $\infty \times N$  ( $\infty \times N'$ ) lattice. This magnitude is used to characterize the different behaviors of the correlation length for the different phases. In general,  $N'=N-1$ , but as explained below, for  $X > 0.5$  we used  $N'=N-4$ .

(iii) Persistence length  $\hat{\xi}$ ,<sup>9</sup>

$$\hat{\xi} = 1 / \ln(\lambda_1 / \lambda_3) . \quad (14)$$

This magnitude is a measure of the interface free energy between the different phases which coexist at a transition line.

(iv) Specific heat,

$$C = -k_B T \frac{\partial^2 f}{\partial T^2} , \quad (15)$$

which was numerically obtained from our data of  $\lambda_1(T)$ . We used 50 values of temperature in each determination. Throughout this paper we use  $k_B T = J_1 / K_1$ , where  $J_1$  is the nearest-neighbor interaction along the  $x$  (or row) direction.

(v) The critical exponent of the correlation length,<sup>8v</sup>

$$\nu = \ln(N/N') / \ln \left[ \frac{\partial(N/\xi_N)}{\partial T} / \frac{\partial(N'/\xi_{N'})}{\partial T} \right]. \quad (16)$$

Additionally, for the ANNNI model we used the correlation function to gain a qualitative understanding of the behavior of the different phases. In this case the rather small lattice sizes we were able to study constitute a serious limitation.

### B. The ANNNI model

It is well known that if  $K_0 > 0$  the ground state of this model for  $X < 0.5$  is ferromagnetic, while for  $X > 0.5$  it is an antiferromagnetic state known as  $\langle 2 \rangle$ , characterized by a periodic arrangement consisting of two up spins followed by two down spins along the  $x$  axis. The spin arrangement along the  $y$  axis is always ferromagnetic. For  $X > 0.5$  the ground state is fourfold degenerate; moreover, as its periodicity is 4, one must use lattices with  $N = 4, 8, 12, \dots$  to avoid introducing artificial interfaces.

#### 1. $X < 0.5$

For  $X < 0.5$  the ordered phase boundaries were determined using phenomenological renormalization.

Figure 1 shows the finite-size behavior of the correlation length for  $X = 0.3$ . It can be observed that the transition temperature is rather insensitive to changes in the lattice size.

On the other hand, the specific heat has a stronger size dependence. If  $X < 0.35$  we found a single phase transition; we show here (Fig. 2) the specific heat for

$X = 0.45$  to exhibit a case with both transitions. Figure 3 shows the scaling function  $Y$  as a function of temperature, for  $X = 0.45$ . It is convenient to study its behavior together with PR (see Fig. 4) for the same data.

We distinguish the following three regions.

(1)  $T < 0.91$ . This corresponds to an ordered phase whose correlation length grows exponentially with  $N$ . We verified that in this case the scaling function grows linearly with  $N$ , in agreement with the expected exponential growth of the correlation length.<sup>11</sup>

(2)  $T = 0.912$ . This phase-transition point is found by means of PR (Fig. 4), but it is interesting to see that it is also clearly shown in the  $Y$ -versus- $T$  curve.

(3) A region where  $Y$  is asymptotically independent of  $N$ . This is consistent with a phase-transition point where the correlation length grows algebraically with  $N$ .

#### 2. $X > 0.5$

For  $X > 0.5$  our results show that there are two phase transitions. At low temperatures we verified that the correlation function shows a behavior consistent with the  $\langle 2 \rangle$  phase; unfortunately, due to the structure of its ground state, we are unable to use the correlation function to study the other phases.

The phase boundaries were determined using PR (see Fig. 5). As a check we used the scaling function for  $N = 12$  (Fig. 6). A true determination of the phase boundaries with this method requires another curve, for instance, for  $N = 16$ . We did not do this, for computational reasons. Of course, we computed  $Y$  for  $N = 8$ , but

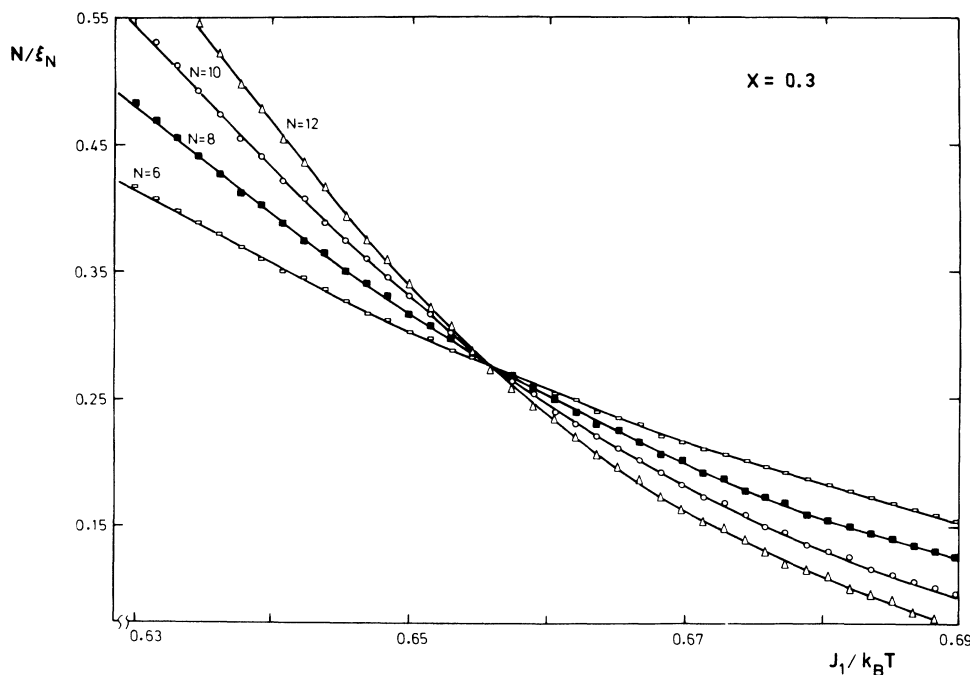


FIG. 1. Inverse correlation length as a function of inverse temperature for the ANNNI model,  $X = 0.3$ . Data for  $N = 5, 7, 9, 11$  are not shown in order to improve the clarity of the figure.

here size effects are too large for this width. Rather, we used the  $N=12$  result by analogy with the behavior shown by the same kind of function for  $X < 0.5$  (Fig. 3). Hence we are assuming that the lower transition happens for  $T < T_A$ , while the second transition occurs around  $T_B$ . These estimates are in close agreement with PR results.

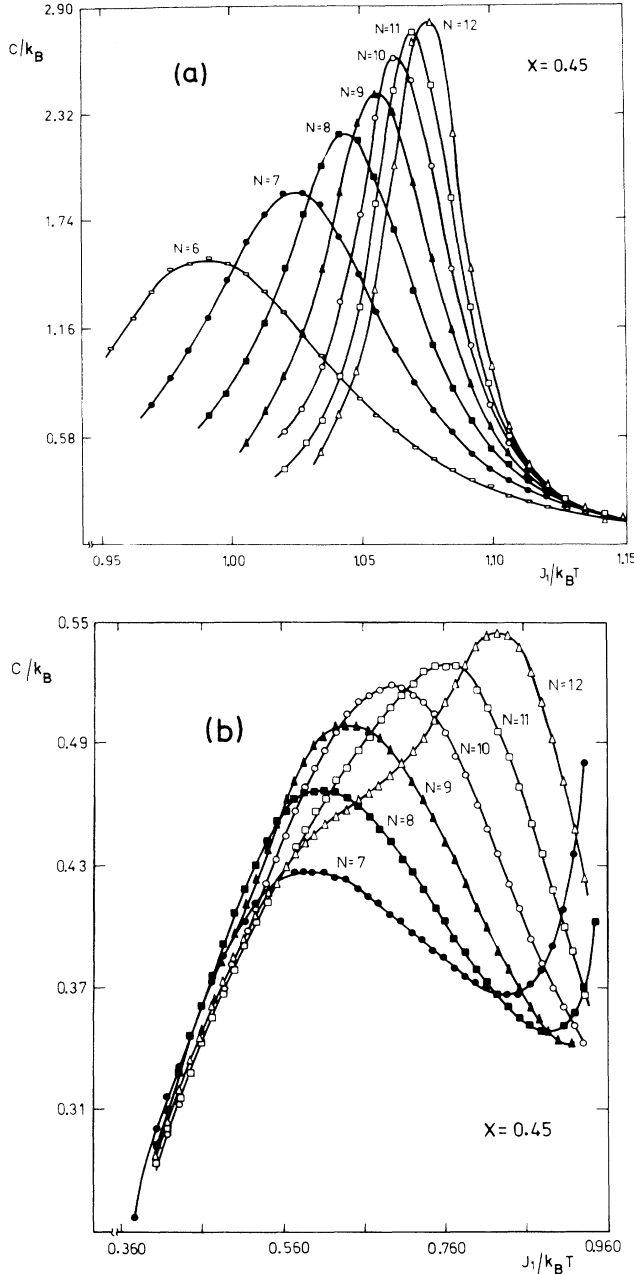


FIG. 2. Specific heat as a function of inverse temperature for the ANNNI model,  $X=0.45$ . In (a) we show the low-temperature transition for  $N=6-12$ . It can be seen that it converges to  $T_c=0.86$ . The behavior at the high-temperature transition (b) is rather different and these data cannot be used to find the value of  $T_c$ , showing that, apparently, size effects are more relevant at the second transition.

### C. The 2+4 model

For  $K_0 > 0$  and  $X < 0.5$ , the ground state of this model is ferromagnetic, while for  $X > 0.5$  it is an octuplet consisting of repeated patterns of spins, such that  $\text{sgn}(s_1 s_2 s_3 s_4) = -1$ :  $(+ - - -)$ ,  $(- + - -)$ ,  $\dots$ ,  $(- + + +)$  along the  $x$  axis.<sup>2</sup> The spin arrangement along the  $y$  axis is always ferromagnetic.

Kolb and Penson<sup>12</sup> used the quantum Hamiltonian approach to study this model in the highly anisotropic limit case  $K_1, K_4 \rightarrow 0$ ,  $K_0 \rightarrow \infty$  with  $h/\gamma_1 = K_1^{-1} \exp(-2K_0)$ ,  $h/\gamma_2 = K_2^{-1} \exp(-2K_0)$ , where  $h$  is a transverse magnetic field and  $\gamma_1$  and  $\gamma_2$  are the quantum interactions, and found that there is only one phase-transition line for all values of  $X$ .

In our case, the determination of the transition point for  $K_0/K_1=1$ , and small values of  $X$ , was almost independent of the size of the sample, as can be seen in Fig. 7, while for  $X$  near 0.5 it has a pronounced dependence with  $N$ . In the neighborhood of  $X < 0.5$  we get a rough estimate of the size dependence comparing critical temperatures obtained with  $N=10$  and 12. We find two different types of behavior, which are best described with the help of the data for  $Y(T)$ . At low temperatures  $Y$  increases linearly with  $N$  (Fig. 8), implying an ordered phase (exponential growth of the correlation length).<sup>11</sup> At high temperatures,  $Y$  decreases exponentially with  $N$ , as is the case for a disordered fluid phase (correlation length asymptotically independent of  $N$ ). At  $T=1.2$  there is a critical point.

There is no evidence of another change, as was the case for the ANNNI model, i.e., we did not find a modulated phase, in agreement with Ref. 12.

### D. Order of the transitions and phase diagrams

The order of the phase transitions was determined with the help of the scaled persistence length<sup>9</sup> in the following form. Once the transition line is determined, we calculate  $\hat{\xi}_N/N$  for several values of  $N$  on this line.

If the scaled persistence length increases with  $N$ , then the transition is first order. If  $\hat{\xi}_N/N$  decreases with  $N$ , the transition is continuous.

For the lowest transition of the ANNNI model we found that  $\hat{\xi}_N/N$  grows with  $N$ , implying that this transition is always first order, except for  $X=0$  (the Ising model). The same result is obtained for 2+4 model (see Fig. 9).

We want to point out, however, that a determination of the critical exponent  $\nu$  for both models and  $X < 0.5$  gives  $\nu=1.00 \pm 0.01$ . Scaling relations then give  $\alpha=2-d\nu=0.00 \pm 0.01$ . This seems to indicate that these transitions belong to the Ising-model universality class, implying that the transitions should be continuous. This is also the main assumption of FSS methods,<sup>13</sup> which for a critical point predict an algebraical growth of the correlation length with  $N$ , as can be observed, for instance, in Fig. 3 (at point L).

A more unreliable determination of  $\alpha$  obtained from the specific-heat data gives a rather large value, suggesting, on the contrary, that the transition could be first order. At the second transition of the ANNNI model,

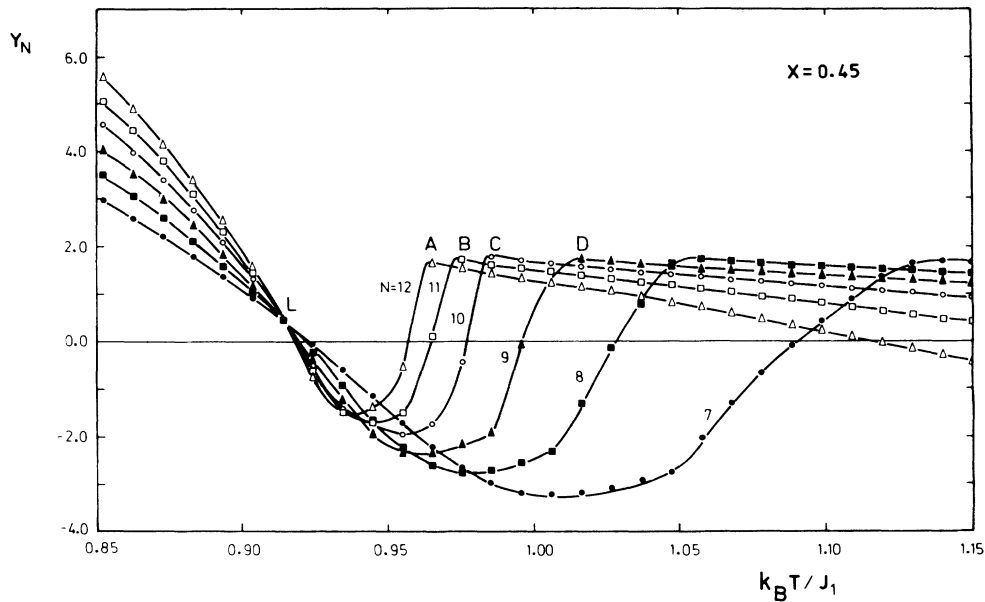


FIG. 3. Scaling function  $Y$  vs  $T$ ,  $X=0.45$ , for the ANNNI model. The system has a phase transition from the low-temperature ferromagnetic phase to an intermediate, short-range-order phase, at point  $L$  ( $T_L=0.912$ ). If  $T < T_L$  the scaling function  $Y$  grows linearly with the width  $N$  of the strip, implying that the correlation length grows exponentially with  $N$ . Points  $D, C, B, A$  are successive estimations of a second phase transition which takes place around  $T_A=0.97$ , from the intermediate- to the high-temperature paramagnetic phase. A qualitative determination of the correlation function in the paramagnetic phase indicates that near  $T_A$  it has an oscillatory behavior superimposed on its exponential decay.

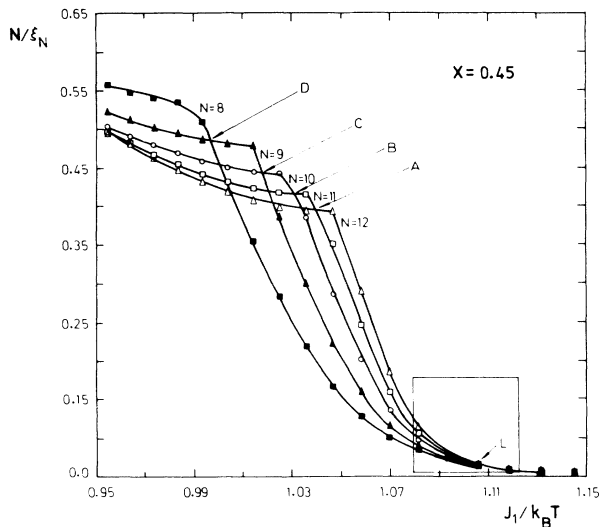


FIG. 4. Inverse scaled correlation length vs inverse temperature for the ANNNI model,  $X=0.45$ . The small region inside the square in the right-hand corner near  $T_L=1.10$  has a behavior similar to that shown in Fig. 1. The phase transition at point  $L$  follows closely that shown in Fig. 3. Points  $D, C, B, A$  are successive approximations of the second transition temperature, as determined by phenomenological renormalization. Note that points  $A-D$  are in correspondence with the same points shown in Fig. 3.

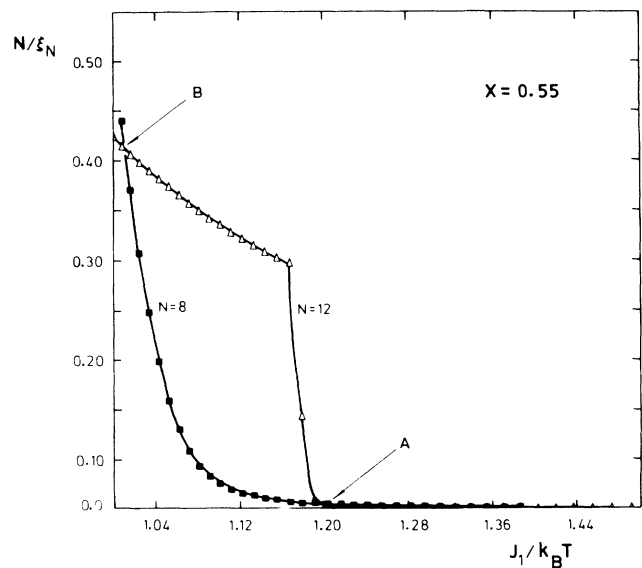


FIG. 5. Inverse correlation length as a function of inverse temperature for the ANNNI model,  $X=0.55$ . For this value of  $X$  it is necessary to use lattices with  $N=4, 8, 12, \dots$  due to the ground-state structure and the use of periodic boundary conditions. Points  $A$  and  $B$  denote our estimate of the first and second transition temperatures.

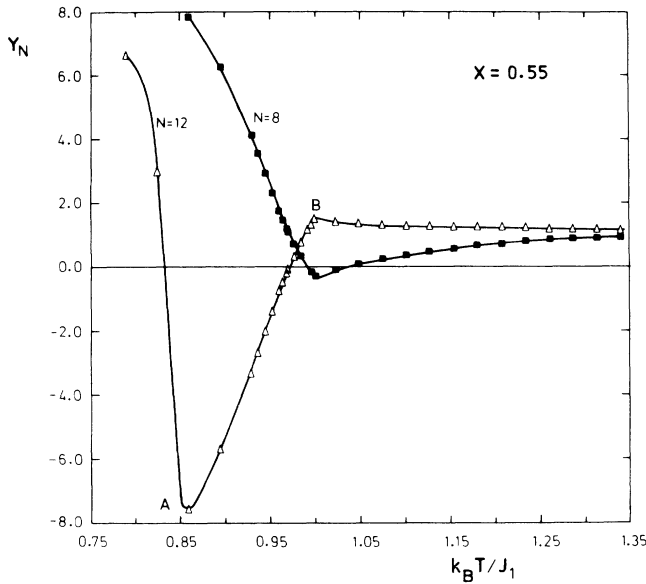


FIG. 6. Scaling function  $Y$  vs temperature,  $X=0.55$ , for the ANNNI model. The estimations of the first and second transition temperatures, points  $A$  and  $B$ , respectively, agree with the determination made in Fig. 5. Size effects are too large to consider the  $N=8$  curve.

$\hat{\xi}_N/N$  decreases with  $N$ , indicating that it is always continuous. All this information is summarized in the phase diagrams of the models (see Figs. 10 and 11).

The ferromagnetic ( $F$ ) and  $\langle 2 \rangle$  phases of the ANNNI model have long-range order. The paramagnetic phase ( $P$ ) has short-range-order correlations; we can distin-

guish in a qualitative form a region without modulation ( $q=0$ ), just above the ferromagnetic phase, and a region with  $q \neq 0$ , above it.

We have been unable to study the intermediate phase for  $X > 0.5$  in any detail, with the exception of the determination of its phase boundaries.

The phase diagrams of the  $2+4$  model has some similarities with the diagram of the ANNNI model, having a ferromagnetic ( $F$ ) and a degenerate phase ( $D$ ) in correspondence with the  $F$  and  $\langle 2 \rangle$  phases of the previous model. On the other hand, we found no evidence of modulated phases or disorder lines, as was the case in the ANNNI model.

As a by-product of our analysis of the behavior of the persistence length preliminary results seem to show that the normalized and scaled persistence length,

$$I_N = [\hat{\xi}_N(K_0, K_1, X)/N] / [\hat{\xi}_{N_0}(K_0, K_1 X)/N_0], \quad (17)$$

scales on the lower transition line, for  $X < 0.5$  and  $K_0/K_1 = 1, 10, 50$ , and  $100$ , for both models. Our results (Fig. 12) show that the phase transition is first order for all these values of the ratio  $K_0/K_1$ . The scaling property is lost for  $X > 0.5$ .

It is perhaps interesting to remark once more that the phase boundaries were determined by the use of FSS methods, the validity of which is widely accepted for continuous transitions. On the other hand, we have used the persistence-length criteria to find regions of these boundaries where the transitions are first order.

This inconsistency is shared with all recent works published on first-order phase transitions studied with

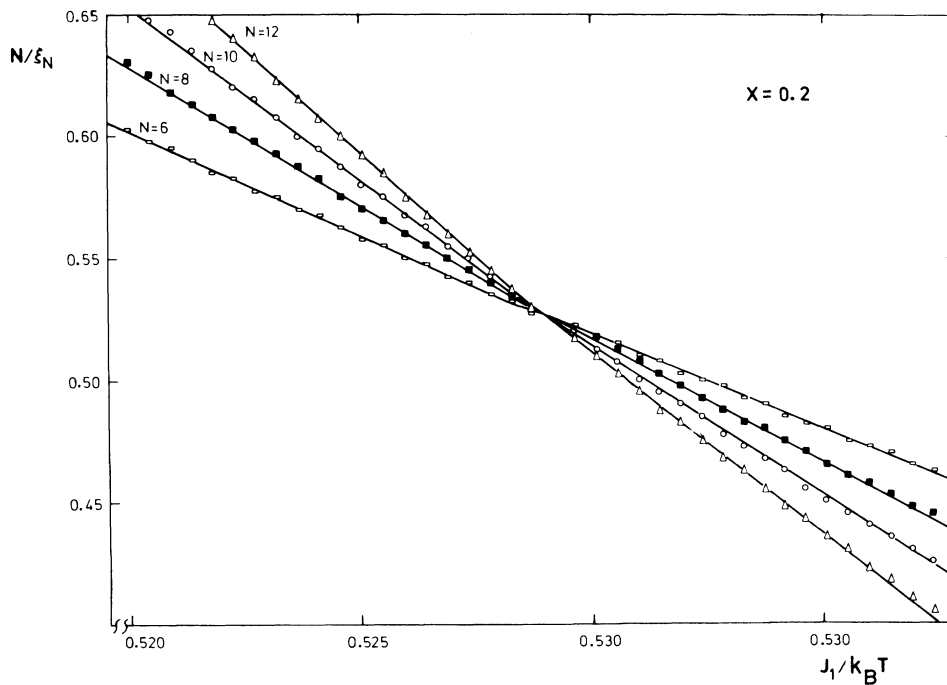


FIG. 7. Inverse correlation length vs inverse temperature for the  $2+4$  model,  $x=0.2$ . Data for  $N=5, 7, 9, 11$  are not shown in order to improve the clarity of the figure.

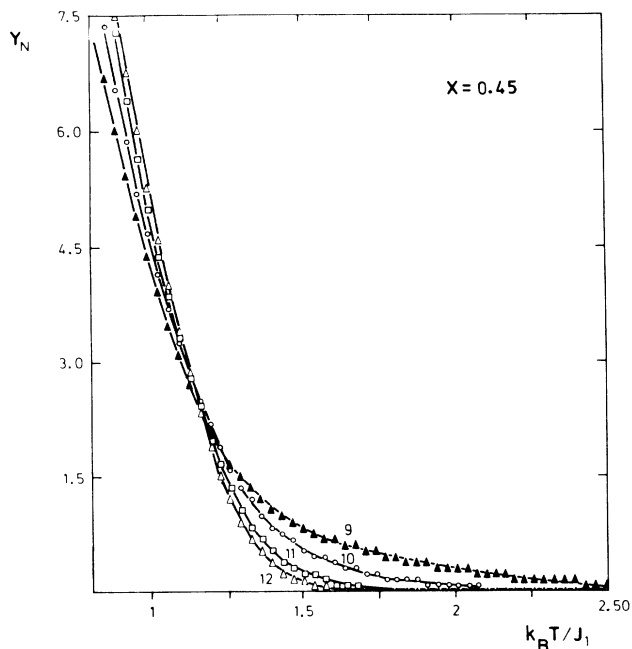


FIG. 8. Scaling function  $Y$  vs temperature  $T$ ,  $X=0.45$ , for the 2+4 model.

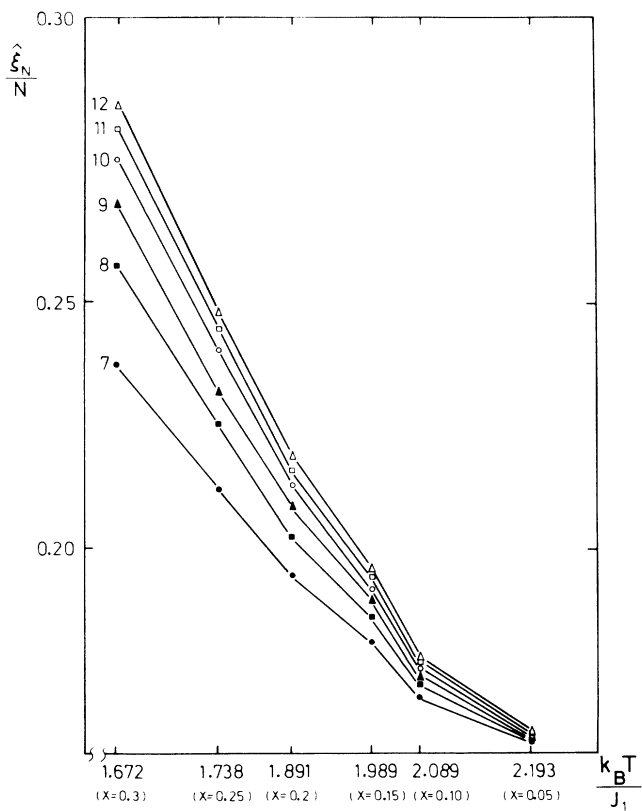


FIG. 9. Scaled persistence correlation length ( $\hat{\xi}_N/N$ ) vs transition temperatures for the 2+4 model. At its lower transition temperature, the ANNNI model exhibits a similar behavior. This figure implies a first-order transition. At  $X=0$  (the Ising model)  $\hat{\xi}_N/N$  decreases with  $N$ , as it should for a continuous transition.

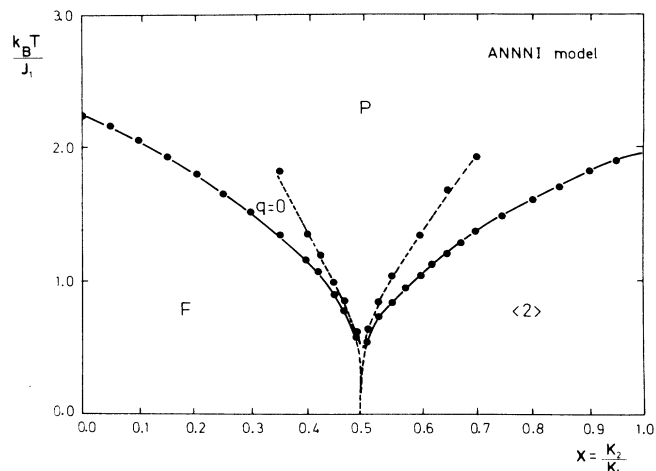


FIG. 10. Phase diagram of the ANNNI model. Size effects are negligible on the lower transition line, and very difficult to estimate along the second transition line.

FSS and PR techniques, and is a point which deserves further investigation.

ACKNOWLEDGMENTS

One of us (M.G.) is grateful to the Consejo Nacional de investigaciones Científicas y Técnicas, Argentina (CONICET) for financial support.

APPENDIX

The purpose of this appendix is to illustrate how the action of the transfer matrix on any row state can be reduced to a simple spin-flip process. We describe the procedure for the ANNNI model, but it can be carried out in the same way for any other model with complex interactions in one direction.

Let  $|\psi\rangle$  be any row state expressed as a linear com-

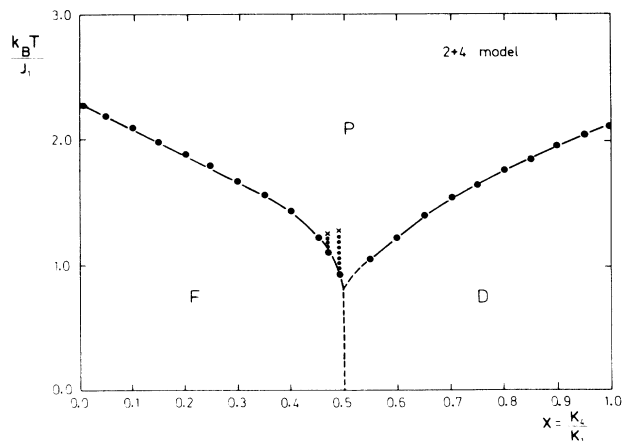


FIG. 11. Phase diagram of the 2+4 model. Size effects are only noticeable around  $X=0.5$ . For  $X=0.47$  and  $0.49$  we also show the transition temperature for  $N=10$  (symbol  $\times$ ) as a rough estimate of the size dependence.

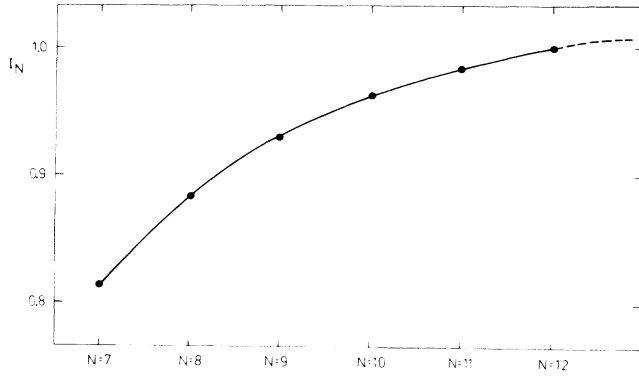


FIG. 12. Normalized scaled persistence length,  $I_N = [\hat{\xi}_N(K_0, K_1, X)/N] / [\hat{\xi}_{N_0}(K_0, K_1, X)/N_0]$ , for  $N_0 = 12$  and  $X = 0.3$ . Data for  $K_0/K_1 = 1, 10, 50$ , and  $100$  on the transition line separating the ferromagnetic and paramagnetic phases for both models, can be fitted by a single curve, showing a scaling property of  $I_N$ . For  $X > 0.5$  we found that this property is lost. The continuous line is only a guide to the eye.

bination of  $2^N$  row states quantized along the  $z$  direction.

$$|\psi\rangle = \sum_{j=1}^{2^N} u_j |\varphi_j\rangle, \quad (\text{A1})$$

where  $|\varphi_j\rangle = |s_{j_1}^z, \dots, s_{j_N}^z\rangle$ .

According to Eq. (8), the transfer matrix of the ANNNI model can be written as

$$\hat{T} = \tilde{V}_0^{1/2} \mathcal{P}_N \tilde{V}_0^{1/2}, \quad (\text{A2})$$

where

$$\begin{aligned} \mathcal{P}_N &= \prod_{n=1}^N P_n, \\ P_n &= 2 \cosh K_0 \cosh K_1 \cosh K_2 \\ &\quad \times (1 + \tanh K_1 \sigma_n^x \sigma_{n+1}^x + \tanh K_2 \sigma_n^x \sigma_{n+2}^x \\ &\quad + \tanh K_1 \tanh K_2 \sigma_{n+1}^x \sigma_{n+2}^x), \end{aligned} \quad (\text{A3})$$

$$\tilde{V}_0^{1/2} = (\tanh K_0)^{\hat{N}/2},$$

and  $\hat{N}$  is the row number operator.  $\hat{N}$  simply counts the number of up spins of any state.

Periodic boundary conditions are expressed as

$$\sigma_{N+1}^x = \sigma_1^x, \quad \sigma_{N+2}^x = \sigma_2^x. \quad (\text{A4})$$

The application of  $\tilde{V}_0^{1/2} = (\tanh K_0)^{\hat{N}/2}$  to any state  $|\psi\rangle$  gives

$$\tilde{V}_0^{1/2} |\psi\rangle = \sum_j u'_j |\varphi_j\rangle, \quad (\text{A5})$$

where  $u'_j = (\tanh K_0)^{n_j/2} u_j$ , and  $n_j$  is the number of up spins of  $|\varphi_j\rangle$ .

The action of any  $P_n$  on an arbitrary state  $|\psi\rangle$  can be written as

$$P_n |\psi\rangle = \sum_j u_j^{(n)} |\varphi_j\rangle, \quad (\text{A6})$$

where

$$\begin{aligned} u_j^{(n)} &= 2 \cosh K_0 \cosh K_1 \cosh K_2 \\ &\quad \times (u_j + \tanh K_1 u_{j(n, n+1)} + \tanh K_2 u_{j(n, n+2)} \\ &\quad + \tanh K_1 \tanh K_2 u_{j(n+1, n+2)}), \end{aligned} \quad (\text{A7})$$

and  $j(n_1, n_2)$  is the index of the row state  $|\varphi_{j(n_1, n_2)}\rangle$  obtained by flipping the spins  $s_{j, n_1}, s_{j, n_2}$  of the row state  $|\varphi_j\rangle$ .

This is clearly seen by remembering that

$$\sigma^x |\uparrow\rangle_z = |\downarrow\rangle_z, \quad \sigma^x |\downarrow\rangle_z = |\uparrow\rangle_z. \quad (\text{A8})$$

Repeating this calculation scheme  $N$  times for each of the  $N$  generated vectors, one can compute the effect of  $\mathcal{P}_N$  on any state  $|\psi\rangle$ .

Applying the operator  $\tilde{V}_0^{1/2}$  again in the way explained above, one can finally compute the total effect of the transfer matrix on any initial state  $|\psi\rangle$ .

To accomplish this purpose it is only necessary to construct a vector  $\mathbf{n} = (n_1, \dots, n_{2^N})$  whose components  $n_j$  are the number of up spins of the  $|\varphi_j\rangle$  state, and a  $2^N \times N$  matrix whose elements  $N_{j,i}$  give the index of the state obtained by flipping the  $s_{j_i}$  spin of the state  $|\varphi_j\rangle$ . Hence, by this method we never need to actually construct the transfer matrix.

Note that the type of interaction of the model is defined in Eq. (A7), which, in our computer program, is merely a simple subroutine.

It is worthwhile to point out that the Lanczös scheme provides not only the leading eigenvalues, but also it is possible to obtain  $|\varphi\rangle_{\max}$ , the eigenvector corresponding to the maximum eigenvalue, and then obtain information about the correlation function.

<sup>1</sup>R. J. Elliot, Phys. Rev. **124**, 346 (1961).

<sup>2</sup>K. A. Penson, Phys. Rev. B **29**, 2404 (1984).

<sup>3</sup>M. Duxbury and M. N. Barber, J. Phys. A **15**, 3219 (1982).

<sup>4</sup>W. Selke and M. E. Fisher, Z. Phys. B **40**, 71 (1980); W. Selke, *ibid.* **43**, 335 (1981); M. N. Barber and W. Selke, J. Phys. A **15**, L617 (1982).

<sup>5</sup>R. M. Hornreich, R. Leibman, H. G. Schuster, and W. Selke,

Z. Phys. B **35**, 91 (1975).

<sup>6</sup>J. Villain and P. Back, J. Phys. (Paris) **42**, 657 (1981).

<sup>7</sup>T. D. Schultz, D. C. Mattis, and E. H. Lieb, Rev. Mod. Phys. **36**, 856 (1964).

<sup>8</sup>P. Nightingale, Physica **83A**, 561 (1976); J. Appl. Phys. **53**, 7927 (1983); M. N. Barber, in *Phase Transitions and Critical Phenomena*, edited by C. Domb and J. Lebowitz (Academic,



- New York, 1983), Vol. 8.
- <sup>9</sup>P. A. Rikvold, W. Kinzel, J. D. Gunton, and K. Kaski, Phys. Rev. B **28**, 2686 (1983); P. D. Beale, *ibid.* **33**, 1717 (1986).
- <sup>10</sup>R. Whitehead, A. Watt, B. J. Cole, and I. Morrison, in *Advances in Nuclear Physics*, edited by M. Baranger and E. Vogt (Plenum, New York, 1977), Vol. 9.
- <sup>11</sup>P. D. Beale, P. Duxbury, and J. Yeomans, Phys. Rev. B **31**, 7166 (1985).
- <sup>12</sup>M. Kolb and K. A. Penson, Phys. Rev. B **31**, 3147 (1985).
- <sup>13</sup>J. Cardy and P. Nightingale, Phys. Rev. B **27**, 4256 (1983), and Ref. 8.